Chemical Science

ROYAL SOCIETY OF CHEMISTRY

EDGE ARTICLE

View Article Online
View Journal

Cite this: DOI: 10.1039/d5sc08693k

All publication charges for this article have been paid for by the Royal Society of Chemistry

Received 8th November 2025
Accepted 23rd December 2025

DOI: 10.1039/d5sc08693k

rsc.li/chemical-science

Chemoselectivity in the cationic Phospha-Wittig reaction: accessing phosphorus heterocycles, phosphaalkenes, and their annulated [4 + 2] dimers

Philipp Royla, [a] Kai Schwedtmann, [a] Rosa M. Gomila, [b] Antonio Frontera [b] and Jan J. Weigand *[a]

Triflate salts of phosphito-phosphanides $[L_CP–P(OR)_3]^+$ (**1**[OTf], R = alkyl, L_C = *N*-heterocyclic carbene) were obtained *via* nucleophilic fragmentation of the tetraphosphetane $[(L_C)_4P_4][OTf]_4$ (**3**$[OTf]_4$) with organophosphites $P(OR)_3$. The salts **1**[OTf] act as versatile reagents in the cationic Phospha-Wittig reaction, converting aldehydes into imidazoliumyl-substituted phosphaalkenes **2**[OTf] and, *via* a competing pathway, into diphosphiranes **4**$[OTf]_2$. The product distribution is governed by the aldehyde substituent, enabling selective access to isolable derivatives of both compound classes. The resulting phosphaalkenes **2**[OTf] serve as precursors to diverse phosphorus heterocycles, undergoing expected [2 + 2] dimerisation to 1,3-diphosphetanes *syn*/*anti*-(**2**)$_2[OTf]_2$ and trapping reactions with 1,3-dienes to yield the tetrahydrophosphinine **8**[OTf] and bicyclic derivative **9**[OTf]. Most notably, an unprecedented annulative [4 + 2] dimerisation pathway for cationic *C*-aryl phosphaalkenes is uncovered that furnishes benzannulated tetrahydro-1,2-diphosphinines **7**$[OTf]_2$. Computational studies reveal that the operative mechanism of this transformation involves a Phospha-Diels–Alder step followed by an acid–base-catalytic proton transfer, which is calculated to be energetically more accessible than the classical [2 + 2] dimerisation.

Introduction

Phosphaalkenes are defined by the presence of a localized phosphorus–carbon double bond (P=C). Despite the electronegativity difference between the two elements, the 2p-3p π-bond in these molecules is nearly apolar,[1] imparting phosphaalkenes with reactivity patterns more closely resembling those of alkenes than imines.[2,3] A small HOMO–LUMO gap in phosphaalkenes confers a unique electronic structure that makes them attractive as scaffolds for transition metal-mediated catalysis and as versatile building blocks in polymer synthesis and organophosphorus chemistry.[2,4–6]

In the absence of sufficient electronic or steric stabilisation, the P=C double bond engages in dimerisation reactions (Fig. 1). The most commonly observed pathway is a [2 + 2] cycloaddition, occurring either in a head-to-head or head-to-tail fashion to furnish 1,2- or 1,3-diphosphetanes **A** or **B**, respectively.[7–11] Alternative dimerisation modes are reported for conjugated 1-phosphabutadienes, which can behave as both dienes and dienophiles in [4 + 2] Phospha-Diels–Alder reactions. Depending on the phosphorus substituent, distinct regioisomeric outcomes are observed. Sterically small

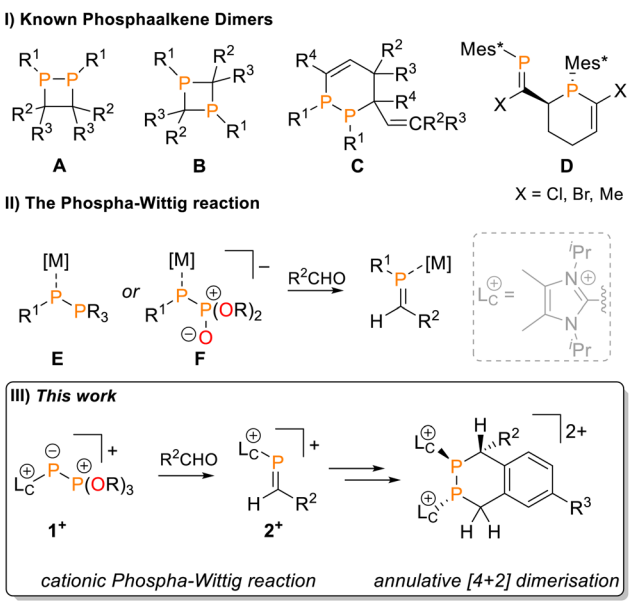

Fig. 1 (I) Known examples of phosphaalkenes and 1-phosphabutadiene dimers; (II) general formula for the Phospha-Wittig reaction, [M] = *e.g.* $[W(CO)_5]$; (III) synthesis of imidazoliumyl-substituted phosphaalkenes 2^+ from phosphito-phosphanides 1^+ and their annulative [4 + 2] dimerisation.

[a]*Faculty of Chemistry and Food Chemistry, Technische Universität Dresden, 01062 Dresden, Germany. E-mail: jan.weigand@tu-dresden*

[b]*Department of Chemistry, Universitat de Illes Balears, 07122 Palma de Mallorca, Spain*

substituents favour P–P bond formation to give diphosphacyclohexenes **C** (R^1 = Me, Cy, ^{t}Bu, Ph),[12,13] whereas the bulky Mes* (Mes* = 2,4,6-^{t}Bu$_3$C$_6$H$_2$) group promotes formation of phosphaalkene-tethered phosphacyclohexenes **D**.[14]

Synthetic access to the P=C motif is achieved by approaches that mirror classical organic transformations used to construct C=C double bonds.[9] A historically important method is the Phospha-Wittig reaction, which involves the transfer of a phosphinidene fragment from phosphanylidene-phosphoranes, R^1P–PR$_3$ or R^1P[M]–PR$_3$ (**E**, M = metal fragment), or -phosphonates, R^1P–P(O)(OR)$_2$ or R^1P[M]–P(O)(OR)$_2$ (**F**, M = metal fragment) to a carbonyl compound (Fig. 1).[15–18]

We are investigating the chemistry of cationic *P*-imidazoliumyl-substituted phosphaalkenes, accessible *via* an adapted route from the reaction of phosphonio-phosphanides [L_CP–PR$_3$]$^+$ (R = aryl, alkyl, L_C = *N*-heterocyclic carbene) with thiocarbonyls.[19] The imidazoliumyl group stabilises the low-coordinated phosphorus environment and simultaneously acts as a leaving group, permitting post-synthetic modification.[20,21] This modularity could provide a general route to tailor phosphaalkenes for specific electronic or steric environments from a common precursor, avoiding optimization of multi-step procedures. However, extending this approach to prepare C–H-functionalised phosphaalkenes **2**$^+$ from aldehydes *via* a cationic Phospha-Wittig reaction was challenging.

The Horner–Wadsworth–Emmons (HWE) reaction offers a compelling alternative to the classical Wittig reaction for the construction of C=C double bonds.[22] This well-established method employs phosphonate-stabilised carbanions, which are more nucleophilic than their ylide counterparts. Indeed, the heavier metal-coordinated phosphorus analogues **F** (Fig. 1) readily react with ketones, while the reactivity of **E** is limited to aldehydes. Inspired by this logic, we targeted phosphito-phosphanides **1**$^+$ and hypothesized that they could react with aldehydes to give access to imidazoliumyl-substituted phosphaalkenes **2**$^+$.

We now report the synthesis of isolable triflate salts of **1**$^+$ *via* the nucleophilic fragmentation of tetraphosphetane [(L_C)$_4$P$_4$][OTf]$_4$ (**3**[OTf]$_4$) by organophosphites P(OR)$_3$ (R = alkyl). Derivatives of **1**$^+$ enable the cationic Phospha-Wittig reaction with a range of aldehydes for the first time. We systematically assess the chemoselectivity of this transformation leading to selective access to isolable phosphaalkenes and diphosphiranes. In addition, we uncover a hitherto unknown [4 + 2] dimerisation pathway of *C*-aryl substituted phosphaalkenes that furnishes benzannulated tetrahydro-1,2-diphosphinines. Computational studies reveal an underlying Phospha-Diels–Alder mechanism succeeded by a proton shift mediated by acid-base catalysis. Crucially, our findings highlight that cationically charged *P*-imidazoliumyl-substituted phosphaalkenes unlock new reactivity profiles that are inaccessible to their neutral counterparts.

Results and discussion

Synthesis of phosphito-phosphanides

Treating **3**[OTf]$_4$ with a slight excess (4.2 equiv.) of organophosphites P(OR)$_3$ (R = Me, Et, ^{i}Pr, Cy) in CH_3CN or CD_2Cl_2 gave pale-yellow solutions after 16 h at room temperature (Scheme 1). In all cases, ^{31}P NMR spectroscopic investigations of aliquots removed from the reaction mixture revealed the complete conversion of **3**[OTf]$_4$. The products displayed the expected AX spin systems with characteristically shielded resonances of the A parts and were assigned to **1a–d**[OTf] [$\delta(^{31}P_A)$ = −199.4–(−182.4) ppm, $\delta(^{31}P_X)$ = 78.3–90.2 ppm, ^1J(PP) = −608–(−601) Hz; see the SI for details, Section S2.1].[19,23]

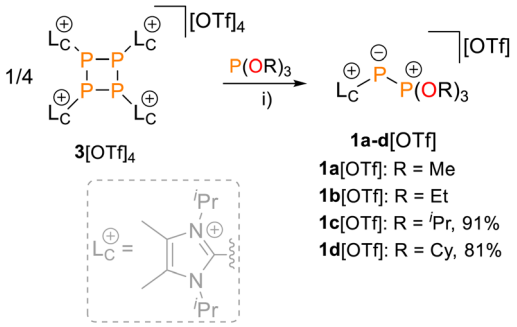

Scheme 1 Nucleophilic fragmentation of **3**[OTf]$_4$ with organophosphites P(OR)$_3$ (R = Me, Et, ^{i}Pr, Cy); reagents and conditions: (i) +4.2 P(OR)$_3$, CH_3CN or CD_2Cl_2, r.t., 16 h, 91% (**1c**[OTf], R = ^{i}Pr), 16 h, 81% (**1d**[OTf], R = Cy).

Whereas work-up of **1a,b**[OTf] led to their decomposition to unidentified products and starting material (see the SI, Fig. S1), analytically pure **1c,d**[OTf] were obtained in isolated yields of 91% and 81%, respectively. Their synthesis is conveniently adaptable to a multigram scale (~3.5 g). Structural confirmation of **1d**[OTf] was achieved through single-crystal X-ray diffraction analysis after recrystallisation from a saturated C_6H_5F/Et_2O solution at room temperature (Fig. 2). The observed P–P bond length [2.0832(5) Å] is markedly shorter than those reported for cationic phosphonio-phosphanides [L_CP–PR$_3$]$^+$ [R = alkyl, 2.1162(4)–2.1446(4) Å][19] and falls at the lower end of the range for structurally characterised phosphanylidene-phosphoranes (2.06–2.15 Å),[23] approaching values characteristic of P=P double bonds (*cf.* P=P 2.04 Å, P–P 2.22 Å).[24,25]

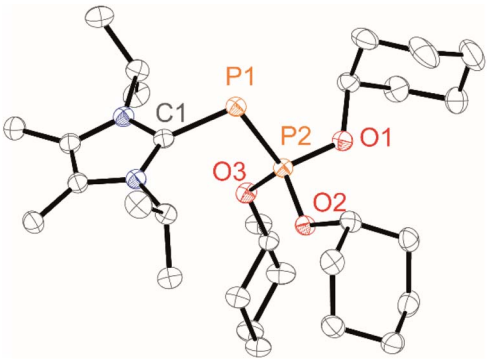

Fig. 2 Molecular structure of **1d**$^+$ in **1d**[OTf]; hydrogen atoms are omitted for clarity, and thermal ellipsoids are displayed at 50% probability (100 K); selected bond lengths (in Å) and angles (in °): P1–P2 2.0832(5), C1–P1 1.8151(16), P2–O1 1.5713(12), P2–O2 1.5764(11), P2–O3 1.5694(11), C1–P1–P2 96.75(5).

Phosphito-phosphanides as Phospha-Wittig reagents

The reactivity of **1c,d**[OTf] was tested in reactions with an excess (2–10 equiv.) of a series of aldehydes R^1CHO in CH_3CN solution (Scheme 2). ^{31}P NMR spectroscopic analysis of aliquots removed from the reaction mixtures after 4 h to 7 d (see Table 1) showed successful Phospha-Wittig conversion to the phosphoric acid esters, $OP(O^iPr)_3$ [$\delta(^{31}P) = -2.8$ ppm][26] or $OP(OCy)_3$ [$\delta(^{31}P) = -2.5$ ppm], and phosphaalkenes *E*-**2a–i**$^+$, indicated by diagnostic, deshielded resonances [$\delta(^{31}P) = 173.8–200.5$ ppm, $^2J(PH) = 14–23$ Hz, see the SI, Fig. S13]. Minor, slightly upfield-shifted [$\delta(^{31}P) = 154.0–176.6$ ppm] resonances were assigned to the corresponding *Z*-isomers due to the characteristically large $^2J(PH)$ coupling constant [$^2J(PH) = 43–44$ Hz].[27] The reactions are highly stereoselective with typical *E*/*Z* ratios > 97 : 3. The ^{31}P NMR resonances of phosphaalkenes **2a–i**$^+$ are shifted to lower frequencies compared to the reported values of neutral C–H substituted phosphaalkenes [$\delta(^{31}P) =$ avg. 250 ppm].[8,16,18,28,29] Similar trends are known for inversely polarized phosphaalkenes.[30]

In addition to phosphaalkenes, the $^{31}P\{^1H\}$ NMR spectra of most reaction mixtures (for **2a–g**$^+$) showed sets of shielded resonances of AX spin systems [*e.g.*, R^1 = Ph (a): $\delta(^{31}P_A) = -174.1$ ppm, $\delta(^{31}P_X) = -138.9$ ppm, $^1J(PP) = 128$ Hz, $^2J(P_XH) = 31$ Hz] in line with the formation of diphosphiranes **4a–g**$^{2+}$ (Scheme 2, for the integral ratio see Table 1).[31] Diphosphirane formation was rationalised by cyclopropanation of the *in situ*–formed phosphaalkenes by phosphinidene $[L_C–P]^+$, transferred from **1c,d**[OTf], in a ligand displacement reaction.[19,32,33] Supporting evidence includes ^{31}P NMR resonances consistent with the transient formation of free $P(O^iPr)_3$ [$\delta(^{31}P) = 140.7$ ppm] over the course of the conversion (see the SI, Fig. S14). In the presence of excess aldehyde, released $P(O^iPr)_3$ is consumed in an Abramov reaction[34] to produce diisopropyl (isopropoxy(aryl) methyl)phosphonates $(^iPrO)_2OP–C(Ar)O^iPr$ [$\delta(^{31}P) =$ *ca.* 25.0 ppm; *cf.* $(MeO)_2OP–C(Ph)OMe$: $\delta(^{31}P) = 21.9$ ppm].[35] Conversion rates of the Phospha-Wittig reaction were accelerated by elevated temperatures, increasing diphosphirane formation, albeit at the expense of lower chemoselectivity, and the formation of several other unidentified products (see the SI, Section S2.6). Notably, while diphosphiranes are typically not observed in the Phospha-Wittig reaction using phosphanylidene-phosphoranes, Gates *et al.* reported diphosphirane formation in the Phospha–Peterson reaction.[8]

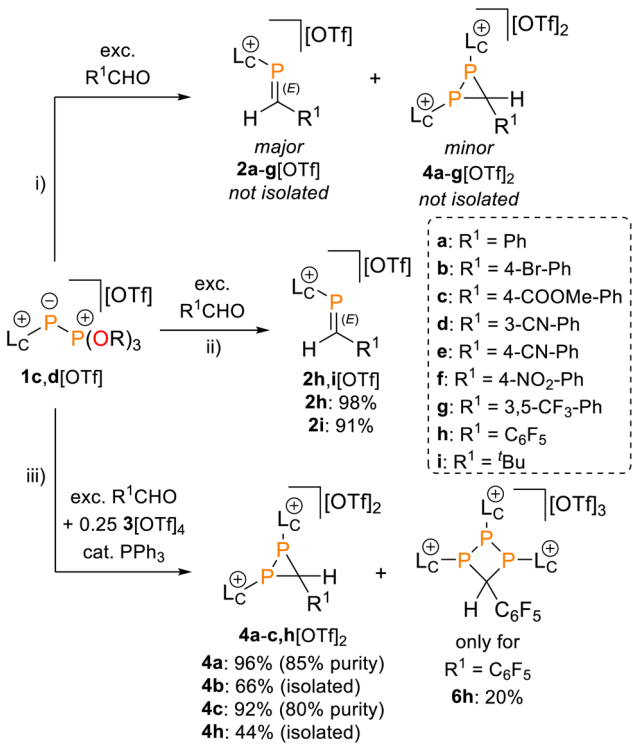

Scheme 2 Reaction of **1c,d**[OTf] with an excess of aldehydes R^1CHO to give inseparable mixtures of **2a–g**[OTf] and **4a–g**$[OTf]_2$ (top) or isolable **2h,i**[OTf] (middle); and direct, independent synthesis of **4a–c**$[OTf]_2$ (bottom); reagents and conditions: (i) + 2.0–5.0 equiv. of R^1CHO, – $OP(OR)_3$, CH_3CN, r.t., 4 h-7 d, 98% (for **2h**[OTf]), 91% (for **2i**[OTf]); (ii) for $R^1 = C_6F_5$: +2.0 equiv. of F_5C_6CHO, $-OP(O^iPr)_3$, CH_3CN, r.t., 4 h, 98%; for $R^1 = {}^t$Bu: +10.0 equiv. of ^{t}BuCHO, $-OP(O^iPr)_3$, CH_3CN, r.t., 4 d, 91%; (iii) for **4a–c**$[OTf]_2$: +5.0 equiv. of R^1CHO, +0.25 equiv. of **3**$[OTf]_4$, +0.1 equiv. of Ph_3P, $-OP(O^iPr)_3$, CH_3CN, r.t., 4 d-7 d, 66% (for **4b**$[OTf]_2$), for **4h**$[OTf]_2$ and **6h**$[OTf]_3$: +2.0 equiv. of F_5C_6CHO, +0.25 equiv. of **3**$[OTf]_4$, +0.1 equiv. of Ph_3P, $-OP(O^iPr)_3$, CH_3CN, r.t., 3 d, 44% (for **4h**$[OTf]_2$) and 20% (for **6h**$[OTf]_3$).

In general, reactions of **1c**[OTf] with aldehydes bearing electron-withdrawing groups or ^{t}BuCHO favoured phosphaalkene formation (see Table 1), while reactions with 4-methoxybenzaldehyde or mesitylaldehyde did not result in satisfactory phosphaalkene or diphosphirane production (see the SI, Section S2.7). Similar solubilities of the triflate salts of phosphaalkenes **2a–g**$^+$ and diphosphiranes **4a–g**$^{2+}$ prevented their separation. However, the phosphaalkenes **2h,i**$^+$ [$R^1 = C_6F_5$ (**2h**$^+$), ^{t}Bu (**2i**$^+$)] were obtained chemoselectively leading to the isolation of their triflate salts in excellent yields of 98% and 91%, respectively. The *E*-configuration of the cations was verified by single-crystal X-ray diffraction analysis (Fig. 3). In the solid state the P=C double bond lengths {**2h**[OTf]: P1–C12 1.692(4) Å, **2i**[OTf]: P1–C12 1.671(2) Å} are similar to other structurally characterised, C–H substituted phosphaalkenes (1.61–1.71 Å),[36] for instance *E*-Mes*P=C(H)Ph [P=C 1.660(6) Å],[29] and close to the calculated values for the parent $HP=CH_2$ [P=C 1.652 Å (at the 6-31G* level of theory)].[37] We also note that the P=C bond in **2h**[OTf] is co-planar with the C_6F_5 substituent, indicating a delocalization of the π-electron density.[9]

The direct and chemoselective formation of the diphosphiranes **4a–c**$^{2+}$ was achieved independently by reacting **1c**[OTf] with the corresponding aldehydes in the presence of 0.25 equivalents of **3**$[OTf]_4$ and catalytic PPh_3, as a source of $[L_C–P]^+$ (Scheme 2). After work-up, the triflate salts **4a,c**$[OTf]_2$ were obtained as crude solids (purity 80–85%, determined by ^{31}P NMR spectroscopy), enabling the unambiguous assignment of all atoms with multinuclear NMR analysis. Efforts to purify these solids by washing with various solvent mixtures, recrystallisation, or separation over a silica plug under inert conditions did not improve purity and in some cases resulted in decomposition to unidentified products. In contrast, diphosphirane **4b**$[OTf]_2$ precipitated as an analytically pure solid from a saturated C_6H_5F solution of the crude product and was isolated in 66% yield.

Table 1 Scope of the Phospha-Wittig reaction of **1c,d**[OTf] with a series of aldehydes

R^1 =		Reagent	Time[a]	Equiv.	$2^+ : 4^{2+}$ ratio	$\delta(^{31}P)$:*E*-2^+, *Z*-2^+ in ppm	$^2J(PH)$:*E*-2^+, *Z*-2^+ in Hz
	**2a**$^+$	**1c**[OTf] **1d**[OTf] **1c**[OTf]	7d 7d 4h[b]	5.0 5.0 5.0	63 : 37 65 : 35 42 : 57	178.2, 154.0	19, 44
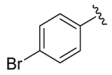	**2b**$^+$	**1c**[OTf]	5d	5.0	79 : 21	182.5, 157.8	21, 43
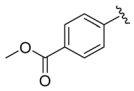	**2c**$^+$	**1c**[OTf]	4d	5.0	83 : 17	191.5, 167.0	22, 44
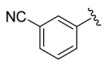	**2d**$^+$	**1c**[OTf]	4d	5.0	91 : 9	192.0, 168.4	22, 43
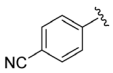	**2e**$^+$	**1c**[OTf]	16h	5.0	91 : 9	197.5, 172.3	20, 43
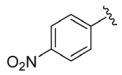	**2f**$^+$	**1c**[OTf]	16h	5.0	92 : 8	200.5, 175.5	22, 43
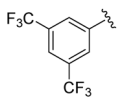	**2g**$^+$	**1c**[OTf]	16h	5.0	94 : 6	200.3, 176.6	23, 43
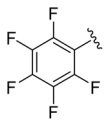	**2h**$^+$	**1c**[OTf]	4h	2.0	>99 : 1	215.5, –	20, –
	**2i**$^+$	**1c**[OTf]	4d	10.0	>99 : 1	173.8, –	14, –

[a] Time required for full conversion of **1c,d**[OTf] at room temperature, if not specified differently. [b] 80 °C.

X-ray diffraction analysis of suitable crystals of **4b**[OTf]$_2$ verified the molecular structure and the *anti*-disposition of the two L_C-substituents (Fig. 3). The central three-membered ring features acute bond angles [*e.g.* P1–C1–P2 73.10(5)°] and C–P bond distances [P1–C1 1.8668(13) Å, P2–C1 1.8729(13) Å], consistent with other structurally identified diphosphiranes.[19,31,33,38] The P1–

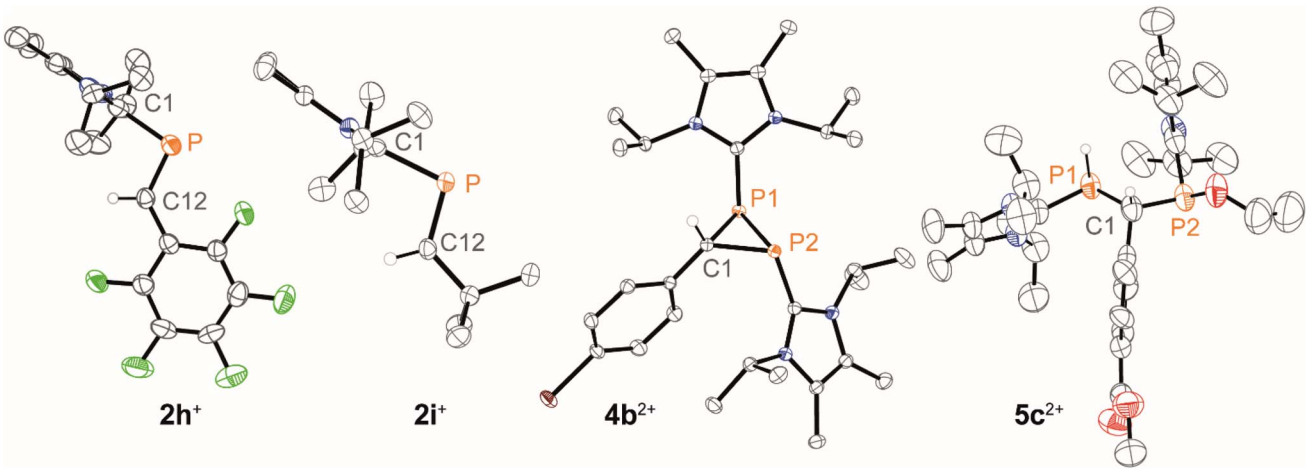

Fig. 3 Molecular structures of **2h,i**$^+$ in **2h,i**[OTf], **4b**$^{2+}$ in **4b**[OTf]$_2$·*o*-$C_6H_4F_2$, and **5c**$^{2+}$ in **5c**[OTf]$_2$·*o*-$C_6H_4F_2$; selected hydrogen atoms and anions are omitted for clarity, and thermal ellipsoids are displayed at 50% probability (100 K); selected bond lengths (Å) and angles (°): for **2h**$^+$: P1–C12 1.692(4), C1–P1–C12 97.71(19); **2i**$^+$: P1–C12 1.671(2), C1–P1–C12 101.38(10); for **4b**$^{2+}$: P1–P2 2.2270(5), P1–C1 1.8668(13), P2–C1 1.8729(13), P1–C1–P2 73.10(5), C1–P1–P2 53.58(4); for **5c**$^{2+}$: P1–C1 avg. 1.916, P2–C1 avg. 1.858, P1–C1–P2 avg. 101.6.

P2 bond length [P1–P2 2.2270(5) Å] is at the longer end of comparable structures.

Diphosphiranes are known to engage in ring opening reactions *via* P–P bond cleavage upon photo- or thermal treatment or in reactions with electro- and nucleophiles.[39] Similarly, crude compound **4c**$[OTf]_2$ activates the O–H bond in EtOH leading to the isolation of **5c**$[OTf]_2$ in 50% yield, verified by analysis of the molecular structure of **5c**$[OTf]_2$ by single crystal X-ray diffraction analysis (Fig. 3). The product was isolated as a mixture of two diastereomers and variable temperature NMR experiments showed no interconversion between them in a range of 240–340 K (see the SI, Fig. S32).

We further conducted experiments of the *in situ*-generated or isolated phosphaalkenes **2h,i**[OTf] with 0.25 equivalents of **3** $[OTf]_4$ and catalytic PPh_3 to access the diphosphiranes **2h,i** $[OTf]_2$. No signs of conversion were observed for $\mathbf{2i}^+$ ($R^1 = {}^t$Bu) after over a week of stirring at room temperature or treatment at elevated temperatures (up to 70 °C). In contrast, the reaction of phosphaalkene $\mathbf{2h}^+$ ($R^1 = C_6F_5$) afforded diphosphirane $\mathbf{4h}^{2+}$ as the major product. Minor amounts of another previously unobserved product showed sets of resonances in agreement with a AX_2 spin system in the $^{31}P\{^{19}F\}$ NMR spectrum (see the SI, Sections S2.14 and S2.15), which led to the tentative assignment of the product as triphosphetane **6h**$[OTf]_3$ (Scheme 2). A crude solid isolated from the mixture contained both products in a 76 : 24 integral ratio. Separation of the products afforded the triflate salts of diphosphirane **4h**$[OTf]_2$ and triphosphetane **6h** $[OTf]_3$ as analytically pure solids in 44% and 20% yield, respectively, with only minimal contamination (<5%) of the other product according to multinuclear NMR analysis. Attempts to bias the product distribution to selectively form **6h** $[OTf]_3$ by performing the reaction with 0.5 equivalents of **3**$[OTf]_4$ did not lead to a meaningful difference in the observed chemoselectivity (see the SI, Section S2.3). Single crystal X-ray diffraction analysis of both products unambiguously confirmed their molecular structures (for **4h**$[OTf]_2$ see the SI, Fig. S49; for **6h**$[OTf]_3$ see Fig. 4). The formation of **6h**$[OTf]_3$ underpins the previously observed capability of **3**$[OTf]_4$ to simultaneously act as a source of $[L_C\text{–}P]^+$ and $[(L_C\text{–}P)_2]^{2+}$.[21,40]

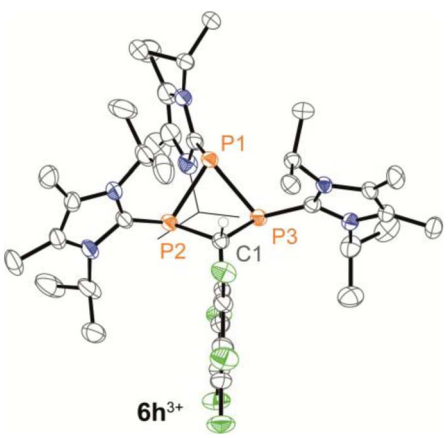

Fig. 4 Molecular structures of $\mathbf{6h}^{3+}$ in **6h**$[OTf]_3 \cdot C_6H_5F$; selected hydrogen atoms and anions are omitted for clarity, and thermal ellipsoids are displayed at 50% probability (100 K), one ^{i}Pr of the L_C group at P1 is shown in wireframe for clarity; selected bond lengths (Å) and angles (°): for $\mathbf{6h}^{3+}$: P1–P2 2.2354(8), P1–P3 2.2540(9), P2–C1 1.890(2), P3–C1 1.904(3), P2–P1–P3 73.56(3), P2–C1–P3 90.24(10).

Dimerisation of imidazoliumyl-phosphaalkenes

While phosphaalkene **2h**[OTf] can be isolated as a monomer from solutions of CH_3CN, colorless precipitates are obtained in solvents of lower polarity, *i.e.* THF or C_6H_5F, after 16 hours at room temperature.

The ^{31}P NMR spectrum of this solid in CH_3CN shows two broadened resonances with low frequencies at $\delta(^{31}P)$ = 19.0 ppm {*anti*-(**2h**)$_2$[OTf]$_2$} and $\delta(^{31}P)$ = −10.9 ppm {*syn*-(**2h**)$_2$[OTf]$_2$} in a 50 : 50 ratio, indicating formation of dimers of $\mathbf{2h}^+$ and loss of P=C double bond character (Scheme 3). Recrystallisation of the solid afforded two sets of colorless crystals suitable for X-ray diffraction analysis, confirming the formation of a *syn*- and *anti*-diastereomer of 1,3-diphosphetane *syn*/*anti*-(**2h**)$_2$[OTf]$_2$, respectively (Fig. 5). The *syn*/*anti* nomenclature refers to the relative position of the transannular imidazoliumyl substituents at the P_2C_2 core. Selected structural parameters are given in Fig. 5. Most importantly, the central P_2C_2 core in *anti*-(**2h**)$_2$[OTf]$_2$ adopts a planar geometry [$\Sigma°(P_2C_2)$ = 360°, C1–P1–C1 86.30(8)°, P1–C1–P2 93.70(8)°], while the P_2C_2 core in *syn*-(**2h**)$_2$[OTf]$_2$ arranges in a butterfly motif with significantly reduced bond angles [C1–P1–C2 avg. 82.07°, P1–C1–P2 avg. 85.95°].

In line with metric parameters found in other structurally characterised 1,3-diphosphetanes, both diastereomers feature long P–C bond lengths [*anti*-(**2h**)$_2$[OTf]$_2$: P1–C1 1.8783(19) Å,

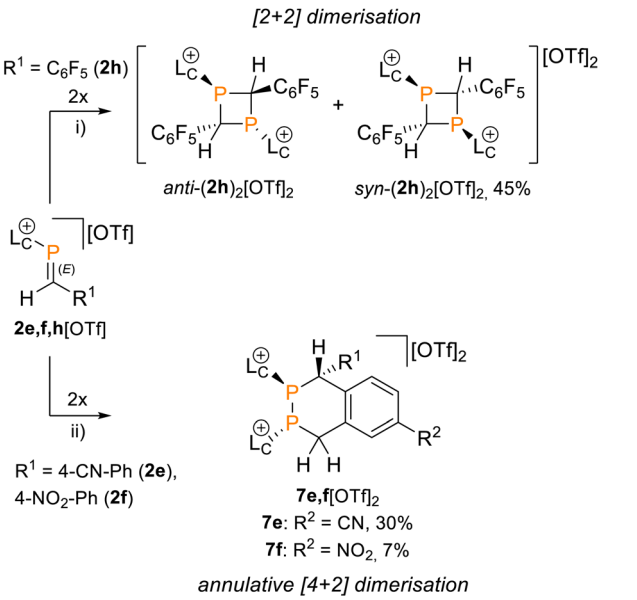

Scheme 3 Formation of *syn*/*anti*-(**2h**)$_2$[OTf]$_2$ *via* [2 + 2] dimerisation of **2h**[OTf] in THF or C_6H_5F and [4 + 2] dimerisation of **2e,f**[OTf] upon work-up to give **7e,f**$[OTf]_2$; reagents and conditions: (i) THF or C_6H_5F, r.t., 16 h, diastereomeric mixture (45% isolated yield for *syn*-(**2h**)$_2$[OTf]$_2$ after fractional recrystallisation); (ii) for **7e**$[OTf]_2$: THF work-up and fractional recrystallisation, r.t., 30%, for **7f**$[OTf]_2$: work-up over a silica plug and fractional recrystallisation, 7%.

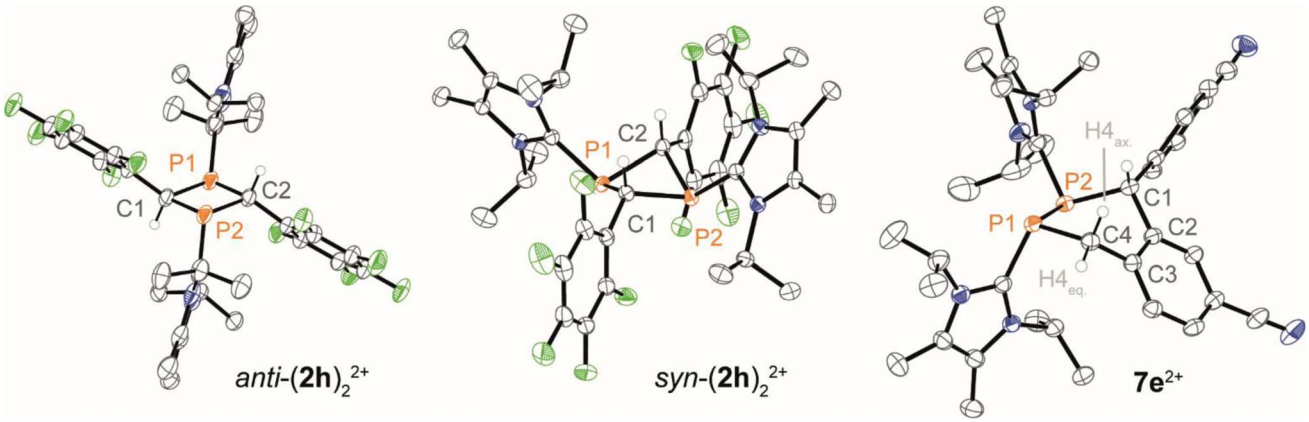

Fig. 5 Molecular structure of *syn*/*anti*-$(\mathbf{2h})_2^{2+}$ in *syn*/*anti*-$(\mathbf{2h})_2[OTf]_2$ and $\mathbf{7e}^{2+}$ in $\mathbf{7e}[OTf]_2\cdot CH_3CN$; hydrogen atoms and anions are omitted for clarity, and thermal ellipsoids are displayed at 50% probability (100 K); selected bond lengths (Å) and angles (°): for *anti*-$(\mathbf{2h})_2^{2+}$: P1–C1 1.8783(19), P1–C2 1.9027(19), C1–P1–C2 86.30(8), P1–C1–P2 93.70(8), P1···P2 2.7586(11); for *syn*-$(\mathbf{2h})_2^{2+}$: P1–C1 avg. 1.891, P1–C2 avg. 1.894, C1–P1–C2 avg. 84.19, P1–C1–P2 avg. 92.82, P1···P2 avg. 2.5724; for $\mathbf{7e}^{2+}$: P1–P2 2.2073(6), P1–C4 1.8636(16), P2–C1 1.8966(17), P1–C4–C3 118.22(12), P2–C1–C2 105.00(11), C1–P1–P2–C4 −25.17(8).

P1–C2 1.9027(19) Å; *syn*-$(\mathbf{2h})_2[OTf]_2$: P1–C1 avg. 1.891 Å, P1–C2 avg. 1.894 Å, *cf.* P–C 1.855 Å[41]] reflecting strained ring systems.[31,33,38] Importantly, this dimerisation is driven by the polarity of the solvent, reflecting another dimension of control for the dimerisation of cationic phosphaalkenes, next to steric and electronic stabilisation of the P=C double bond. Although representatives of 1,3-diphosphetanes have been structurally verified in both configurations,[10,11,19,42] to the best of our knowledge $(\mathbf{2h})_2[OTf]_2$ is the first 1,3-diphosphetane for which both diastereomers are characterised by single crystal X-ray diffraction. Isolated *syn*-$(\mathbf{2h})_2[OTf]_2$ was obtained upon fractional recrystallisation and only mixed fractions were obtained for *anti*-$(\mathbf{2h})_2[OTf]_2$. No interconversions between the diastereomers or to the monomer were observed in a temperature range from 240–340 K using multinuclear NMR spectroscopy (see the SI, Fig. S61).

Attempts to isolate the phosphaalkenes $\mathbf{2e,f}^+$ from their reaction mixtures led to the serendipitous formation of annulated tetrahydro-1,2-diphosphinines $\mathbf{7e,f}[OTf]_2$ (Scheme 3), which were obtained as crude solids in up to 85% ($\mathbf{7e}[OTf]_2$, 80–90% purity) and 58% yield ($\mathbf{7f}[OTf]_2$, 95% purity), respectively. The main impurities of the crude compounds were identified as the respective 1,3-diphosphetanes *syn*/*anti*-$(\mathbf{2e,f})_2[OTf]_2$ and the formation of *syn*-$(\mathbf{2e})_2[OTf]_2$ could be verified crystallographically (see the SI, Fig. S65). Analytically pure samples of $\mathbf{7e,f}[OTf]_2$ were obtained by recrystallisation of the crude products, allowing the confirmation of their molecular structures by single crystal X-ray diffraction analysis (Fig. 5 and S84 in the SI). In the solid state the central six-membered ring of $\mathbf{7e}^{2+}$ adopts a distorted boat conformation with *anti*-oriented imidazoliumyl substituents. Bond lengths and angles are as expected. Notably, the P–P bond distance [2.2073(6) Å] is consistent with a P–P single bond ($\Sigma r_{cov.}$ = 2.22 Å),[24] the only other structurally characterised annulated tetrahydro-1,2-diphosphinine [P–P 2.2072(7) Å],[43] and monocyclic 1,2,3,6-tetrahydrodiphosphinines.[44,45] The diastereoselective formation of the stereogenic centers at P1, P2 and C1 in $\mathbf{7e,f}[OTf]_2$ is supported by single sets of ^{31}P NMR resonances that were iteratively fitted to AB spin systems [$\mathbf{7e}^{2+}$ (CD_2Cl_2, 300 K): exp., $\delta(^{31}P_{AB})$: centered at −51.1 ppm; iteratively fitted, $\delta(^{31}P_A)$ = −52.2 ppm, $\delta(^{31}P_B)$ = −50.4 ppm, $^1J(PP)$ = −190 Hz; $\mathbf{7f}^{2+}$ (CD_3CN, 300 K): exp., $\delta(^{31}P_{AB})$: centered at −53.2 ppm; $\delta(^{31}P_A)$ = −55.8 ppm, $\delta(^{31}P_B)$ = −52.2 ppm, $^1J(PP)$ = −193 Hz]. Additionally, the diastereotopic H4 protons are anisochronous at 300 K [$\mathbf{7e}^{2+}$: $\delta(^1H4_{ax})$ = 4.52 ppm, $\delta(^1H4_{eq})$ = 3.70 ppm, $^2J(HH)$ = 15.1 Hz, $\mathbf{7f}^{2+}$: $\delta(^1H4_{ax})$ = 4.16 ppm, $\delta(^1H4_{eq})$ = 3.84 ppm, $^2J(HH)$ = 15.6 Hz], consistent with the absence of detectable conformational changes in solution (for details see the SI, Section S2.17 and S2.18). The diastereoselective formation of the six-membered ring in $\mathbf{7e,f}^{2+}$ suggests a [4 + 2] dimerisation *via* a Phospha-Diels–Alder type reaction to be the operative pathway. Although auto-Phospha-Diels–Alder processes have been reported for 1-phosphabutadienes[12–14] and 2*H*-phospholes[46] they are elusive to *C*-aryl substituted phosphaalkenes as interactions of P=C double bonds with arenes are exceedingly rare.[47] To rationalize this unusual reactivity we performed quantum chemical calculations (at the RI-BP86-D4/def2-TZVP level of theory) on the formation of $\mathbf{7e}^{2+}$ from two molecules of $\mathbf{2e}^+$, using a truncated imidazoliumyl substituent for computational efficiency (Fig. 6).

The reaction initiates with a concerted annulative [4 + 2] dimerisation of two molecules of $\mathbf{2e}^+$, proceeding through transition state TS1 with a low activation barrier of 12.1 kcal mol^{-1}. The resulting adduct INT1 is nearly isoenergetic with the reactants ($\Delta G°$ = +0.8 kcal mol^{-1}), consistent with a reversible first step. Frontier orbital analysis (see the SI, Fig. S96) supports a normal-electron-demand Phospha-Diels–Alder process, where the HOMO is delocalized over the P=C and C=C bonds (diene) and the LUMO localizes on the P=C unit (dienophile).[48,49]

From INT1, two mechanistic scenarios were evaluated. An intramolecular 1,3 H shift *via* transition state TS2′ is kinetically inaccessible, with a barrier of 38.9 kcal mol^{-1}. In contrast, an acid-base pathway mediated by the triflate counterion proved highly favourable. The acidic aryl C–H bond in INT1,

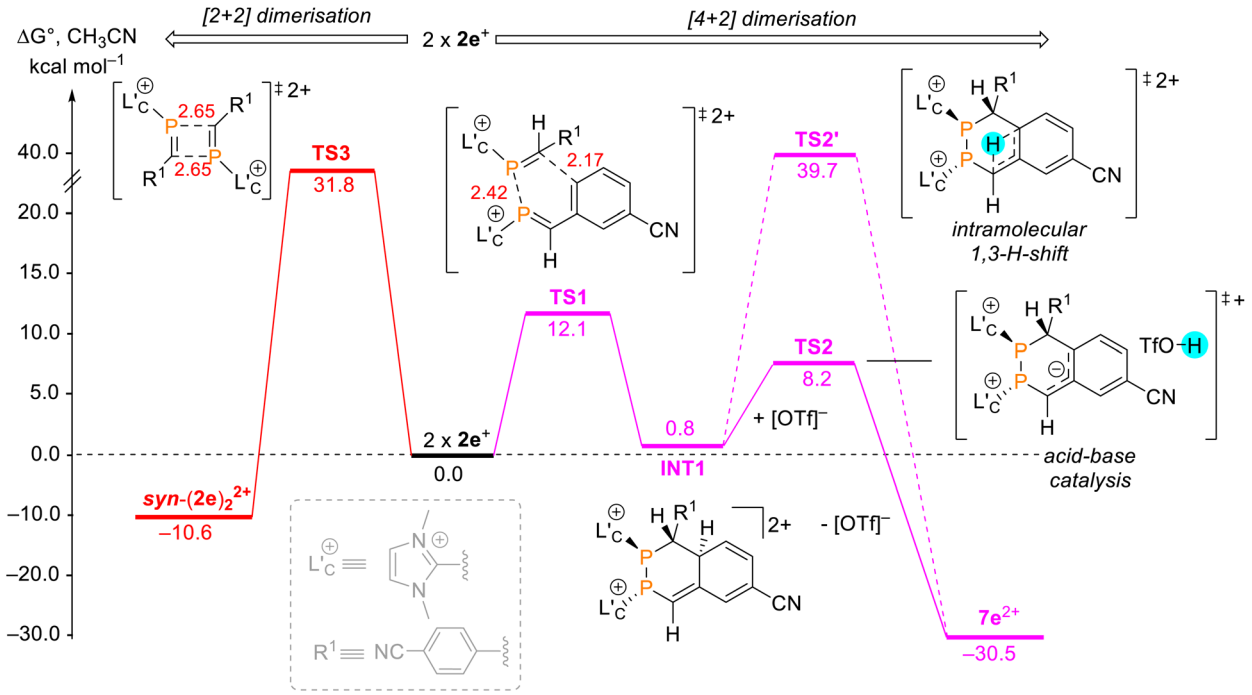

Fig. 6 Calculated free energy profile (Δ*G*°, RI-BP86-D4/def2-TZVP, COSMO = CH_3CN) for the transformation of two equiv. of **2e**$^+$ to **7e**$^{2+}$ *via* a [4 + 2] dimerisation followed by acid-base catalysis (magenta pathway). For comparison, the competing [2 + 2] dimerisation to form *syn*-(**2e**)$_2^{2+}$ (red pathway) is also shown. All energies are reported in kcal mol^{-1} and are relative to two isolated molecules of **2e**$^+$. A truncated model for the imidazoliumyl substituent was used for all calculations.

destabilised by the electron-withdrawing cyano substituents and overall dicationic framework, is readily deprotonated by [OTf]$^-$ (or another weak base in the reaction mixture), giving transition state TS2 ($\Delta G^{\circ\ddagger}$ = 8.2 kcal mol^{-1}). Subsequent reprotonation at the benzylic position occurs barrierless, directly yielding **7e**$^{2+}$, which is strongly stabilised at −30.5 kcal mol^{-1} relative to the starting materials. For comparison, the competing head-to-tail [2 + 2] dimerisation was calculated to be less favourable, with transition state TS3 at 31.8 kcal mol^{-1} for the formation of the corresponding 1,3-diphosphetane *syn*-(**2e**)$_2^{2+}$. Although the product is thermodynamically stable (ΔG° = −10.6 kcal mol^{-1}), the high kinetic barriers render its formation pathway less viable. Notably, the calculations predict the formation of 1,2-diphosphetane to be more feasible than the 1,3-isomer (see the SI, Fig. S97). This discrepancy, along with the generally high absolute values of some calculated barriers (>30 kcal mol^{-1}), is attributed to steric and electronic effects not fully captured by the truncated imidazoliumyl substituent used in the computational model. The preference for the annulative pathway is consistent with dominant formation of **7e,f**[OTf]$_2$ under the mild workup conditions used for **2e,f**[OTf].

Trapping reactions with 1,3-dienes

The Phospha-Diels–Alder reaction is an important tool to demonstrate the existence of thermodynamically unstable phosphaalkenes.[5,6,17,49,50]

In this context, phosphaalkene **2f**$^+$ was trapped in reactions with dienes, namely 2,3-dimethylbuta-1,3-diene (2,3-DMB) and 1,3-cyclohexadiene (1,3-CHD), affording the *anti*-1,2,5,6-tetrahydrophosphinine **8f**$^+$ and *endo*-phosphabicyclo[2.2.2]oct-5-ene **9f**$^+$, respectively (Scheme 4). Both products were isolated as their triflate salts in excellent yields (92% and 91%), and their molecular structures were confirmed by single-crystal X-ray diffraction analysis (Fig. 7). The solid-state structures show the expected *anti* arrangement of the L_C- and 4-NO_2-phenyl substituent in line with the dominant *E*-configuration of **2f**$^+$.

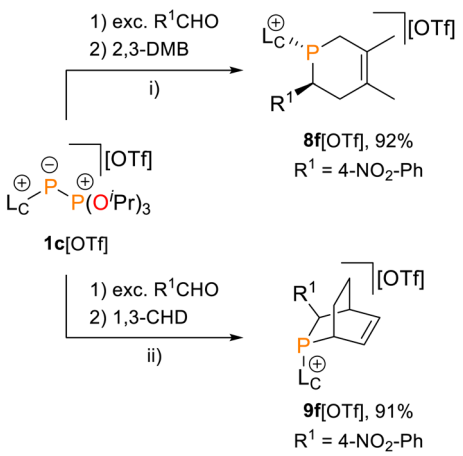

Scheme 4 Phospha-Diels–Alder type trapping reactions of *in situ* prepared imidazoliumyl-substituted phosphaalkene **2f**[OTf] with 2,3-dimethylbuta-1,3-diene (2,3-DMB) and 1,3-cyclohexadiene (1,3-CHD); reagents and conditions: (i) – OP(O^{i}Pr)$_3$, CH_2Cl_2, r.t., 16 h, 92%; (ii) – OP(O^{i}Pr)3, CH_2Cl_2, r.t., 16 h, 91%.

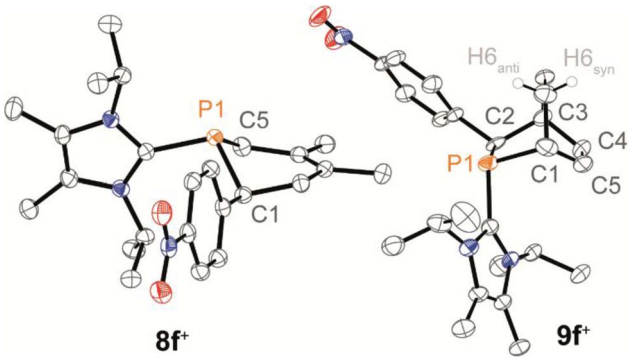

Fig. 7 Molecular structures of $\mathbf{8f}^+$ and $\mathbf{9f}^+$ in **8f**[OTf] and **9f**[OTf]; selected hydrogen atoms and anions are omitted for clarity, and thermal ellipsoids are displayed at 50% probability (100 K); selected bond lengths (Å) and angles (°): for $\mathbf{8f}^+$: P1–C1 1.854(2), P1–C5 1.8341(2), C1–P1–C5 96.9(1); for $\mathbf{9f}^+$: P1–C2 1.869(2), P1–C1 1.882(4), C2–C3 1.575(5), P1–C1–C5 111.4(3), P1–C3–C4 109.9(3).

Bond lengths and angles fall within the expected ranges [*e.g.*, $\mathbf{8f}^+$: P1–C1 1.854(2) Å, $\mathbf{9f}^+$: P1–C2 1.869(2) Å, *cf.* P–C 1.855 Å],[41] and compare well with structurally related 1,2,3,6-tetrahydrodiphosphinines and diphosphabicyclo[2.2.1]hept-5-enes.[45] Compound $\mathbf{9f}^+$ was identified as the *endo*-diastereomer, and multinuclear NMR spectroscopic investigation supports a diastereoselective formation of both products (see the SI for details, Section S2.20). For instance, the ^{31}P NMR spectra of both heterocycles display only a single resonance at 300 K [$\mathbf{8f}^+$: $\delta(^{31}\mathrm{P}) = -47.6$ ppm; $\mathbf{9f}^+$: $\delta(^{31}\mathrm{P}) = -29.9$ ppm].

Conclusions

To conclude, we present a scalable synthesis of (imidazoliumyl) phosphito-phosphanides **1c,d**[OTf] *via* nucleophilic fragmentation of tetraphosphetane **3**$[\mathrm{OTf}]_4$. These reagents facilitate the cationic Phospha-Wittig reaction with a broad range of aldehydes for the first time, providing previously inaccessible *P*-imidazoliumyl-substituted and C–H functionalised phosphaalkenes **2**[OTf]. These phosphaalkenes exhibit rich and chemoselective cycloaddition reactivity. They undergo: (I) [2 + 1] cyclopropenation reaction with cationic phosphinidene $[\mathrm{L_C{-}P}]^+$ transfer reagents to afford the diphosphiranes **4**[OTf] as well as rare triphosphetane **6h**$[\mathrm{OTf}]_3$; (II) solvent-polarity-controlled [2 + 2] head-to-tail dimerisation to yield 1,3-diphosphetanes $(\mathbf{2})_2[\mathrm{OTf}]_2$; (III) Phospha-Diels–Alder reactions with 1,3-dienes to tetrahydrophosphinine **8f**[OTf] and phosphabicyclo[2.2.2]oct-5-ene **9f**[OTf]; and (IV) a hitherto unknown annulative [4 + 2] dimerisation pathway of **2e,f**[OTf], furnishing benzannulated tetrahydro-1,2-diphosphinines **7e,f**$[\mathrm{OTf}]_2$. Mechanistic studies reveal that this transformation proceeds through an auto-Phospha-Diels–Alder step followed by a counter anion-guided proton-transfer and re-aromatisation sequence.

Collectively, these findings significantly expand the reactivity landscape of *C*-aryl-substituted phosphaalkenes and demonstrate that the cationic charge in *P*-imidazoliumyl phosphaalkenes unlocks new synthetic pathways inaccessible to their neutral analogues, a concept that could provide a blueprint for other transformations in main group chemistry. The new cationic heterocycles presented here are promising platforms for post-functionalisation, and further studies in this direction are underway and will be reported separately.

Author contributions

P. R., K. S., and J. J. W. conceptualized the study; P. R. conducted the experiments and optimized the syntheses, isolations, and purifications; R. G. and A. F. were responsible for mechanistic studies; P. R. and J. J. W. were responsible for X-ray data collection and refinement; K. S. and J. J. W. conceived, oversaw, and directed the project; P. R. prepared the initial draft of the paper; A. F. and J. J. W. secured funding. All authors contributed to data analysis, manuscript review and editing, and discussion.

Conflicts of interest

There are no conflicts to declare.

Data availability

Additional data can be obtained from the corresponding author upon reasonable request.

CCDC 2501246–2501257, 2517773 and 2517774 contain the supplementary crystallographic data for this paper.[51a–n]

Supplementary information (SI): the data supporting the findings of this study, including CIF files, NMR spectra, and computational details. See DOI: https://doi.org/10.1039/d5sc08693k.

Acknowledgements

This work was supported by the German Science Foundation (DFG; WE 4621/6–1 and WE 4621/6-2). P. R. thanks the Fonds der Chemischen Industrie (Kekulé scholarship). A. F. and R. G. M. thank MICIU/AEI from Spain for financial support, project PID2023-148453NB-I00, FEDER funds. We also thank Technische Universität Dresden (TUD) for financial support.

Notes and references

1 W. W. Schoeller, *J. Chem. Soc., Chem. Commun.*, 1985, **334**, DOI: 10.1039/C39850000334.
2 F. Mathey, *Angew Chem. Int. Ed. Engl.*, 2003, **42**, 1578.
3 P. Le Floch, *Coord. Chem. Rev.*, 2006, **250**, 627.
4 D. P. Gates, Expanding the Analogy Between P=C and C=C Bonds to Polymer Science, *Springer Berlin Heidelberg*, 2005, **250**(250), 107.
5 K. B. Dillon, F. Mathey and J. F. Nixon, *Phosphorus. The carbon analogy: from organophosphorus to phospha-organic chemistry*, Wiley, Chichester, New York, 1998.
6 R. Appel, ed *Multiple Bonds and Low Coordination in Phosphorus Chemistry*, Thieme, Stuttgart, 1990.
7 (*a*) N. H. T. Huy, L. Ricard and F. Mathey, *Organometallics*, 1988, **7**, 1791; (*b*) A. I. Arkhypchuk, M.-P. Santoni and S. Ott, *Organometallics*, 2012, **31**, 1118; (*c*) A. I. Arkhypchuk,

N. D'Imperio, J. A. L. Wells and S. Ott, *Chem. Sci.*, 2022, **13**, 12239; (*d*) N. D'Imperio, A. I. Arkhypchuk, J. Mai and S. Ott, *Eur. J. Inorg. Chem.*, 2019, **2019**, 1562; (*e*) G. Becker, M. Rssler and W. Uhl, *Z. Anorg. Allg. Chem.*, 1981, **473**, 7; (*f*) G. Becker, W. Uhl and H.-J. Wessely, *Z. Anorg. Allg. Chem.*, 1981, **479**, 41; (*g*) H. Grützmacher and H. Pritzkow, *Angew Chem. Int. Ed. Engl.*, 1992, **31**, 99.

8 S. Wang, K. Samedov, S. C. Serin and D. P. Gates, *Eur. J. Inorg. Chem.*, 2016, **2016**, 4144.

9 M. Yam, J. H. Chong, C.-W. Tsang, B. O. Patrick, A. E. Lam and D. P. Gates, *Inorg. Chem.*, 2006, **45**, 5225.

10 G. Becker and O. Mundt, *Z. Anorg. Allg. Chem.*, 1980, **462**, 130.

11 G. Becker, W. Massa, O. Mundt and R. Schmidt, *Z. Anorg. Allg. Chem.*, 1982, **485**, 23.

12 R. Appel, F. Knoch and H. Kunze, *Chem. Ber.*, 1984, **117**, 3151.

13 G. Martin and E. Ocando-Mavarez, *Heteroat. Chem.*, 1991, **2**, 651.

14 K. Ohtsuki, H. T. G. Walsgrove, Y. Hayashi, S. Kawauchi, B. O. Patrick, D. P. Gates and S. Ito, *Chem. Commun.*, 2020, **56**, 774.

15 (*a*) S. Shah and J. Protasiewicz, *Coord. Chem. Rev.*, 2000, **210**, 181; (*b*) S. Shah, M. C. Simpson, R. C. Smith and J. D. Protasiewicz, *J. Am. Chem. Soc.*, 2001, **123**, 6925; (*c*) S. Shah, T. Concolino, A. L. Rheingold and J. D. Protasiewicz, *Inorg. Chem.*, 2000, **39**, 3860; (*d*) P. Le Floch and F. Mathey, *Synlett*, 1990, **1990**, 171; (*e*) A. Marinetti, S. Bauer, L. Ricard and F. Mathey, *Organometallics*, 1990, **9**, 793; (*f*) P. Le Floch, A. Marinetti, L. Ricard and F. Mathey, *J. Am. Chem. Soc.*, 1990, **112**, 2407; (*g*) T. L. Breen and D. W. Stephan, *J. Am. Chem. Soc.*, 1995, **117**, 11914; (*h*) A. I. Arkhypchuk, Y. V. Svyaschenko, A. Orthaber and S. Ott, *Angew Chem. Int. Ed. Engl.*, 2013, **52**, 6484; (*i*) K. Esfandiarfard, A. I. Arkhypchuk, A. Orthaber and S. Ott, *Dalton Trans.*, 2016, **45**, 2201.

16 S. Shah and J. D. Protasiewicz, *Chem. Commun.*, 1998, 1585.

17 A. Marinetti and F. Mathey, *Angew Chem. Int. Ed. Engl.*, 1988, **27**, 1382.

18 C. C. Cummins, R. R. Schrock and W. M. Davis, *Angew Chem. Int. Ed. Engl.*, 1993, **32**, 756.

19 P. Royla, K. Schwedtmann, Z. Han, J. Fidelius, D. P. Gates, R. M. Gomila, A. Frontera and J. J. Weigand, *J. Am. Chem. Soc.*, 2023, **145**, 10364.

20 (*a*) J. Fidelius, K. Schwedtmann, S. Schellhammer, J. Haberstroh, S. Schulz, R. Huang, M. C. Klotzsche, A. Bauzá, A. Frontera, S. Reineke and J. J. Weigand, *Chem*, 2024, **10**, 644; (*b*) K. Schwedtmann, G. Zanoni and J. J. Weigand, *Chem.–Asian J.*, 2018, **13**, 1388.

21 P. Royla, K. Schwedtmann, R. M. Gomila, A. Frontera and J. J. Weigand, *Angew Chem. Int. Ed. Engl.*, 2025, **64**, e202419502.

22 W. S. Wadsworth and W. D. Emmons, *J. Am. Chem. Soc.*, 1961, **83**, 1733.

23 J. D. Protasiewicz and C. Hering-Junghans, in *Encyclopedia of inorganic and bioinorganic chemistry*, ed R. A. Scott, Wiley, Chichester, 2012, vol. 13, pp. 1–27.

24 P. Pyykkö and M. Atsumi, *Chem.–Eur. J.*, 2009, **15**, 186.

25 P. Pyykkö and M. Atsumi, *Chem.–Eur. J.*, 2009, **15**, 12770.

26 Y. Chen, Y.-F. Zhao, Y.-W. Yin and X.-Q. Yang, *Phosphorus, Sulfur, and Silicon Relat. Elem.*, 1991, **61**, 31.

27 O. Kühl, *Phosphorus-31 NMR Spectroscopy*, Springer Berlin Heidelberg, Berlin, Heidelberg, 2009.

28 (*a*) J. I. Bates, B. O. Patrick and D. P. Gates, *New J. Chem.*, 2010, **34**, 1660; (*b*) M. Brym, C. Jones, M. Waugh, E. Hey-Hawkins and F. Majoumo, *New J. Chem.*, 2003, **27**, 1614; (*c*) J. D. Masuda, K. C. Jantunen, O. V. Ozerov, K. J. T. Noonan, D. P. Gates, B. L. Scott and J. L. Kiplinger, *J. Am. Chem. Soc.*, 2008, **130**, 2408; (*d*) M. Yoshifuji, K. Toyota and N. Inamoto, *Tetrahedron Lett.*, 1985, **26**, 1727.

29 M. Yoshifuji, K. Toyota, I. Matsuda, T. Niitsu, N. Inamoto, K. Hirotsu and T. Higuchi, *Tetrahedron*, 1988, **44**, 1363.

30 L. Weber, *Eur. J. Inorg. Chem.*, 2000, **2000**, 2425.

31 G. Etemad-Moghadam and M. Koenig, in *Phosphorus-Carbon Heterocyclic Chemistry*, Elsevier, 2001, pp. 57–86.

32 (*a*) R. Streubel, N. H. T. Huy and F. Mathey, *Synthesis*, 1993, **1993**, 763; (*b*) G. Etemad-Moghadam, J. Bellan, C. Tachon and M. Koenig, *Tetrahedron*, 1987, **43**, 1793; (*c*) K. Lammertsma and M. J. M. Vlaar, *Eur. J. Inorg. Chem.*, 2002, **2002**, 1127.

33 R. Streubel, M. Nieger and E. Niecke, *Chem. Ber.*, 1993, **126**, 645.

34 R. Engel, in *Organic Reactions*, ed S. E. Denmark, Wiley, 2004, pp. 175–248.

35 I. J. Colton, D. Yin, P. Grochulski and R. J. Kazlauskas, *Adv. Synth. Catal.*, 2011, **353**, 2529.

36 M. Regitz, ed. *Multiple Bonds and Low Coordination in Phosphorus Chemistry*, Thieme, Stuttgart, 1990.

37 M. Yoshifuji, K. Toyota, N. Inamoto, K. Hirotsu, T. Higuchi and S. Nagase, *Phosphorus Sulfur Silicon Relat. Elem.*, 1985, **25**, 237.

38 M.-L. Y. Riu, A. K. Eckhardt and C. C. Cummins, *J. Am. Chem. Soc.*, 2022, **144**, 7578.

39 (*a*) M. Gouygou, C. Tachon, G. Etemad-Moghadam and M. Koenig, *Tetrahedron Lett.*, 1989, **30**, 7411; (*b*) M. Gouygou, C. Tachon, M. Koenig, A. Dubourg, J. P. Declercq, J. Jaud and G. Etemad-Moghadam, *J. Org. Chem.*, 1990, **55**, 5750; (*c*) R. El-Ouatib, C. Garot, G. Etemad-Moghadam and M. Koenig, *J. Org. Chem.*, 1992, **436**, 169; (*d*) M. J. Herve, G. Etemad-Moghadam, M. Gouygou, D. Gonbeau, M. Koenig and G. Pfister-Guillouzo, *Inorg. Chem.*, 1994, **33**, 596; (*e*) M. Gouygou, M. Veith, C. Couret, J. Escudié, V. Huch and M. Koenig, *J. Org. Chem.*, 1996, **514**, 37.

40 (*a*) K. Trabitsch, S. Hauer, K. Schwedtmann, P. Royla, J. J. Weigand and R. Wolf, *Inorg. Chem. Front.*, 2025, **12**, 2013; (*b*) K. Schwedtmann, J. Haberstroh, S. Roediger, A. Bauzá, A. Frontera, F. Hennersdorf and J. J. Weigand, *Chem. Sci.*, 2019, **10**, 6868.

41 W. M. Haynes, D. R. Lide and T. J. Bruno, *CRC Handbook of Chemistry and Physics*, CRC Press, 2016.

42 G. Becker and O. Mundt, *Z. Anorg. Allg. Chem.*, 1978, **443**, 53.

43 A. N. Chernega, M. Y. Antipin, Y. T. Struchkov, V. P. Kukhar', I. V. Shevchenko, O. I. Kolodyazhnyi and I. E. Boldeskul, *J. Struct. Chem.*, 1984, **25**, 280.

44 J. Grobe, A. Armbrecht, D. Le Van, B. Krebs, J. Kuchinke, M. Läge and E.-U. Würthwein, *Z. Anorg. Allg. Chem.*, 2001, **627**, 1241.
45 A. Beil, R. J. Gilliard and H. Grützmacher, *Dalton Trans.*, 2016, **45**, 2044.
46 (*a*) T. Möller, M. B. Sárosi and E. Hey-Hawkins, *Chem.–Eur. J.*, 2012, **18**, 16604; (*b*) P. Wonneberger, N. König, F. B. Kraft, M. B. Sárosi and E. Hey-Hawkins, *Angew Chem. Int. Ed. Engl.*, 2019, **58**, 3208; (*c*) F. Mathey, *Acc. Chem. Res.*, 2004, **37**, 954.
47 L. L. Liu, J. Zhou, L. L. Cao, Y. Kim and D. W. Stephan, *J. Am. Chem. Soc.*, 2019, **141**, 8083.
48 M. Abbari, P. Cosquer, F. Tonnard, Y. Y. C. Y. L. Ko and R. Carrié, *Tetrahedron*, 1991, **47**, 71.
49 H. T. Teunissen, J. Hollebeek, P. J. Nieuwenhuizen, B. L. M. van Baar, F. J. J. de Kanter and F. Bickelhaupt, *J. Org. Chem.*, 1995, **60**, 7439.
50 (*a*) R. de Vaumas, A. Marinetti, L. Ricard and F. Mathey, *J. Am. Chem. Soc.*, 1992, **114**, 261; (*b*) H. Grützmacher and H. Pritzkow, *Angew Chem. Int. Ed. Engl.*, 1989, **28**, 740; (*c*) L. Chen, S. Wang, P. Werz, Z. Han and D. P. Gates, *Heteroat. Chem.*, 2018, **29**, e21474; (*d*) T. van der Knaap and F. Bickelhaupt, *Tetrahedron*, 1983, **39**, 3189; (*e*) P. Le Floch, D. Carmichael and F. Mathey, *Organometallics*, 1991, **10**, 2432.
51 (*a*) CCDC 2501246: Experimental Crystal Structure Determination, 2025, DOI: 10.5517/ccdc.csd.cc2pyrcs; (*b*) CCDC 2501247: Experimental Crystal Structure Determination, 2025, DOI: 10.5517/ccdc.csd.cc2pyrdt; (*c*) CCDC 2501248: Experimental Crystal Structure Determination, 2025, DOI: 10.5517/ccdc.csd.cc2pyrfv; (*d*) CCDC 2501249: Experimental Crystal Structure Determination, 2025, DOI: 10.5517/ccdc.csd.cc2pyrgw; (*e*) CCDC 2501250: Experimental Crystal Structure Determination, 2025, DOI: 10.5517/ccdc.csd.cc2pyrhx; (*f*) CCDC 2501251: Experimental Crystal Structure Determination, 2025, DOI: 10.5517/ccdc.csd.cc2pyrjy; (*g*) CCDC 2501252: Experimental Crystal Structure Determination, 2025, DOI: 10.5517/ccdc.csd.cc2pyrkz; (*h*) CCDC 2501253: Experimental Crystal Structure Determination, 2025, DOI: 10.5517/ccdc.csd.cc2pyrl0; (*i*) CCDC 2501254: Experimental Crystal Structure Determination, 2025, DOI: 10.5517/ccdc.csd.cc2pyrm1; (*j*) CCDC 2501255: Experimental Crystal Structure Determination, 2025, DOI: 10.5517/ccdc.csd.cc2pyrn2; (*k*) CCDC 2501256: Experimental Crystal Structure Determination, 2025, DOI: 10.5517/ccdc.csd.cc2pyrp3; (*l*) CCDC 2501257: Experimental Crystal Structure Determination, 2025, DOI: 10.5517/ccdc.csd.cc2pyrq4; (*m*) CCDC 2517773: Experimental Crystal Structure Determination, 2025, DOI: 10.5517/ccdc.csd.cc2qhyhp; (*n*) CCDC 2517774: Experimental Crystal Structure Determination, 2025, DOI: 10.5517/ccdc.csd.cc2qhyjq.